B1 paper

by Vilia Paramita

Submission date: 22-Apr-2023 02:47AM (UTC-0400)
Submission ID: 2072014510
File name: B1_FH_Journal.pdf (3.59M)
Word count: 7284
Character count: 39110

Food Hydrocolloids 139 (2023) 108555

Contents lists available at ScienceDirect

Food Hydrocolloids

journal homepage: www.elsevier.com/locate/foodhyd

Mechanical *vs* calorimetric glass transition temperature in the oxidation of linoleic acid from condensed κ-carrageenan/glucose syrup systems

Diah Ikasari [a], Vilia Darma Paramita [b], Stefan Kasapis [a,*]

[a] School of Science, RMIT University, Bundoora West Campus, Plenty Road, Melbourne, Vic, 3083, Australia
[b] Department of Chemical Engineering, State Polytechnic of Ujung Pandang, Tamalanrea, Makassar, 90245, Indonesia

ARTICLE INFO

Keywords:
κ-carrageenan
Glucose syrup
Linoleic acid oxidation
Mechanical glass transition temperature

ABSTRACT

Lipid oxidation remains a concern leading to deterioration of the organoleptic quality in processed goods, but it should be minimized by considering changes in the structural properties of foods. The present work investigates the effect of glass transition temperature on the oxidation of linoleic acid at different concentrations of κ-carrageenan/glucose syrup. A combination of 0.5, 1, 2 and 3% (w/w) κ-carrageenan and 82.5, 82, 81, 80% (w/w) glucose syrup were mixed with 1.5% (w/w) linoleic acid and 0.5% (w/w) lecithin to prepare samples with a total solid content of 85% (w/w). Physicochemical properties of these mixtures were recorded using Fourier transform infrared spectroscopy (FTIR) and scanning electron microscopy (SEM). This was followed by estimation of the mechanical (T_{gm}) and calorimetric (T_{gc}) glass transition temperatures using small deformation dynamic oscillation in-shear and modulated differential scanning calorimetry (MDSC). The linoleic acid oxidation in the condensed polysaccharide/co-solute system was evaluated by monitoring the accumulation of hydroperoxide (ROOH) with UV–vis spectroscopy over a wide temperature range (−25 to 0 °C). The oxidation phase was modelled following a sigmoidal kinetic model indicating initiation and propagation stages of lipid oxidation. ROOH production increased as a function of time and temperature. The structural relaxation of the polymeric matrix influenced the oxidation rate at the initiation stage. At the propagation phase, T_{gm} appears to control the rate of ROOH formation (k_f) and decomposition (k_d) in all preparations, as compared to T_{gc}, an outcome that makes the former an important concept of quality control.

1. Introduction

The utilisation of polyunsaturated fatty acids (PUFA) in the human diet has been continuously expanding due to dietary guideline recommendations to supplant saturated lipids (Nogueira, Scolaro, Milne, & Castro, 2019). An issue related to utilising unsaturated lipids in foods is their high susceptibility to free radical-induced lipid peroxidation, which increases with the degree of unsaturation (Domínguez et al., 2019). Among the polyunsaturated fatty acids, linoleic acid, i.e. an omega-6 fatty acid, is essential for human metabolism. It possesses a 18:2n-6 chemical structure consisting of more than one cis double bonds that make it highly vulnerable to lipid oxidation (Saini & Keum, 2018). This vulnerability during storage of processed foods, often leads to the formation of fatty acid peroxides that may cause damage to the structure of adjacent proteins and enzymes (Marangoni et al., 2020).

In general, the oxidation process in polyunsaturated fatty acids occurs rapidly following three successive stages of initiation, propagation and termination (Toorani & Golmakani, 2021). Identification and subsequent quantification of compounds derived from oxidation reactions at each stage is the focus of current research since it can affect distinctly the quality of vegetable oils. Oxidisable substrates may yield high levels of hydroperoxides (ROOHs), which are the first compounds of lipid peroxidation and possess specific significance as the precursor of secondary lipid oxidation products, e.g. aldehydes (hexanal), ketones, alcohols or pentyl furans (Domínguez et al., 2019).

Accumulation of ROOHs at different stages and transfer phases of lipid oxidation can be interpreted by a sigmoidal kinetic model that involves several indices of convenient quality control. These include the rate constant of the initiation phase (k_1), the rate constant of the pseudo first-order formation of ROOHs (k_f) at the propagation phase and the rate constant of the pseudo second-order decomposition of ROOHs (k_d) at the propagation phase (Farhoosh, 2018). Combining observations of the aforementioned indices from the sigmoidal model with the structural characteristics of lipids and the ensuing physicochemical events can

* Corresponding author.
E-mail address: stefan.kasapis@rmit.edu.au (S. Kasapis).

https://doi.org/10.1016/j.foodhyd.2023.108555
Received 3 November 2022; Received in revised form 26 January 2023; Accepted 2 February 2023
Available online 3 February 2023
0268-005X/

provide valuable information that potentially retards the oxidation phase transfer in processed formulations, e.g. commercially baked goods and fast foods.

High-solid food systems often consist of amorphous components that transform from the rubbery to the glassy state upon rapid cooling at the so-called glass transition temperature (T_g) (Fan & Roos, 2017). Above T_g, reaction rates increase dramatically due to the accelerated molecular mobility of the polymeric matrix and the bioactive reactant (Fan & Roos, 2017). Using the concept of the mechanical glass transition temperature (T_{gm}), it was proposed that the structural characteristics of a starch network are critical considerations of the enzymatic activity of the entrapped α-amylase in the polysaccharide matrix (Chaudhary, Panyoyai, Small, Shanks, & Kasapis, 2018). It has been reported in the literature that the variation in T_{gm} is related to the ability of the biopolymer to form a network, a process which rheology is extremely well qualified to follow. In contrast, calorimetry provides information primarily on the mobility of the small-molecule "sugar" co-solute as a function of the total level of solids (Kasapis, 2006; Kasapis, Al-Marhoobi, & Mitchell, 2003). Vitrified materials may also retard the formation of hydroperoxides in encapsulated rapeseed oil by entrapping the hydrophilic and lipophilic radicals (Orlien, Andersen, Sinkko, & Skibsted, 2000). Further studies have reported on the oxidation rate of bulk vegetable oils and encapsulated fish oil particles without a reference to the structural properties of polymeric carriers (Linke, Weiss, & Kohlus, 2020; Nogueira et al., 2019; Toorani & Golmakani, 2021).

Polysaccharides such as carrageenan can form cohesive three-dimensional structures in the presence of cross-linking counterions. Fani, Enayati, Rostamabadi, & Falsafi (2022) have reported on the encapsulation of bioactive compounds by electrosprayed κ-carrageenan nanoparticles. Paramita, Bannikova, & Kasapis (2015) modelled the release mechanism of omega-3 fatty acids in κ-carrageenan/polydextrose matrices undergoing glass transition. The present investigation adds to literature by dealing with the effect of the glass transition temperature on the oxidation state of linoleic acid from condensed κ-carrageenan/glucose syrup systems. These were prepared by varying the concentrations of the polysaccharide and co-solute in the presence of cross-linking potassium counterions. The fatty-acid oxidation rate was examined by employing the kinetic sigmoidal model discussed earlier and outcomes were correlated with the vitrification properties of these systems. Thus, observations on the physicochemical and morphological characteristics of the polymeric matrix were recorded to provide a valid correlation between the dynamics of glass transition mechanism and the oxidation kinetics of the entrapped bioactive lipid that may lead to a better control of organoleptic quality in related food applications.

2. Materials and methods

2.1. Materials

κ-Carrageenan type III, extracted from *Eucheuma cottonii*, was obtained from Sigma–Aldrich (Sydney, Australia), while glucose syrup, with a total solid level of 81% (w/w) and a dextrose equivalent of 42, was supplied by Edlyn Foods (Victoria, Australia). Linoleic acid (99% purity, $M_w \approx 280.45$ kDa) was purchased from Sigma–Aldrich. Lecithin (emulsifier) was purchased from Melbourne Food Ingredient Depot (Melbourne, Australia). Potassium chloride (KCl), Amberlite IR-120 resin, and reagents for the oxidation analysis i.e. chloroform ($CHCl_3$), methanol (CH_3OH), 1-butanol ($CH_4CH_{10}O$), ammonium thiocyanate (CH_4N_2S), barium chloride ($BaCl_2$) and iron (II) sulfate heptahydrate ($FeSO_4.7H_2O$) were all purchased from Sigma-Aldrich. Deionised Milli-Q Type II water was used throughout experimentation. Cumene hydroperoxide (80%) from Sigma-Aldrich was used to produce the standard curve for ROOH determination.

2.2. Sample preparation

A model system composed of κ-carrageenan/glucose syrup with linoleic acid and lecithin at a total solid of 85% (w/w) was prepared. κ-Carrageenan was first converted into the potassium form following the method applied by Ikasari, Paramita, & Kasapis (2022). This was conducted by soaking 200 g Amberlite IR-120 resin in 0.1 M HCl until pH reached 1, followed by submersion of the resin in 2M KCl solution to convert H^+ to K^+ form. The remaining salt was washed away with water until the filtrate showed a clear solution when titrated with $AgNO_3$. The temperature of the resin was then elevated to 90 °C and stirred with 0.5% (w/w) κ-carrageenan for 30 min to perform the ion exchanging process to the potassium form. The κ-carrageenan solution was then dialysed using cellulose-based semi-permeable tubes (height: 20 cm; diameter: 4.3 cm) by submersing in Milli-Q water overnight at ambient temperature. The polysaccharide solution was freeze-dried and used for the following experimentation.

Samples were prepared in a beaker by mixing 0.5, 1, 2, and 3% (w/w) κ-carrageenan in the potassium form with 82.5, 82, 81, and 80% (w/w) glucose syrup, followed by addition of 1.5% (w/w) linoleic acid and 0.5% (w/w) lecithin. In doing so, κ-carrageenan was dissolved in Milli-Q water with constant stirring at 90 °C for 10 min, followed by the incorporation of glucose syrup as the co-solute at 60 °C. The temperature was further reduced to 50 °C, and 1.5% (w/w) linoleic acid as the bioactive compound and 0.5% (w/w) lecithin were added with gentle stirring to reach a total solid of 85% (w/w). Finally, 200 mM of KCl was added to the mixture at this temperature. In the end, beakers were covered with a plastic wrap and further sealed with aluminium foil to prevent exposure to environmental conditions. They were kept in a refrigerator before further analysis.

2.3. Experimental analysis

2.3.1. Fourier transform infrared spectroscopy

Interferograms were recorded using Spectrum Two GladiATR-Fourier transform infrared spectroscopy (PerkinElmer, Pike Technologies, Norwalk, US) following the method used by Panyoyai, Bannikova, Small, & Kasapis (2015). Condensed samples of single glucose syrup, linoleic acid and tertiary systems consisting of κ-carrageenan, glucose syrup and fatty acid were scanned at a wavelength of 700–4000 cm^{-1} with 4 cm^{-1} resolution based on 64 average scans. Experimental results were subtracted from the background solvent signal, and each sample was prepared separately and analysed three times.

2.3.2. Scanning electron microscopy

In the presence of 200 mM KCl, single systems of glucose syrup and κ-carrageenan were compared to the mixture of κ-carrageenan, glucose syrup, linoleic acid and lecithin. The working protocol followed the method by Paramita et al. (2015) with some modifications. Samples were freeze-dried, coated with iridium, and subjected to the intense electron beam and high vacuum conditions of 0.6 Torr using FEI Quanta 200 SEM (Hillsboro, Oregon, USA). High-quality images of the samples were captured at an average of 10.2 mm working distance and magnification of 3000–6000 ×, using an accelerated medium voltage of 30 kV and a spot size of 5.

2.3.3. Modulated differential scanning calorimetry

Measurements of the thermal profile were performed by using Q2000 (TA Instruments, New Castle, DE) with a refrigerated cooling system (RCS90). About 10 mg of samples were placed into T_{zero} aluminium pans, sealed hermetically and subjected to experimentation against an empty pan, which served as the reference. Measurements were run under nitrogen purge at a rate of 50 ml/min. Samples were equilibrated at 20 °C for 20 min, followed by cooling from 20 to −90 °C at a scan rate of 1 °C/min and heating to 80 °C at the same scan rate with a modulation rate of 0.53 °C for every 40s (Rahman, 2009). The glass

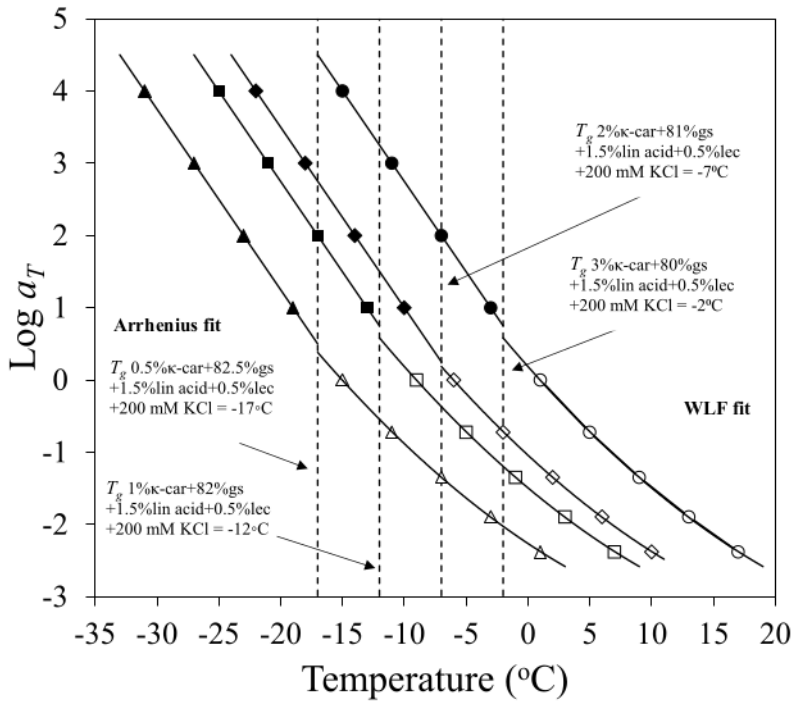

Fig. 6. WLF and modified Arrhenius fits of the shift factors (a_T) within the glass transition region (open symbols) and glassy state (closed symbols) for 0.5% κ-car +82.5% gs +1.5% lin acid+0.5% lec+200 mM KCl (triangle), 1% κ-car+82% gs+1.5% lin acid +0.5% lec+200 mM KCl (square), 2% κ-car+81% gs+1.5% lin acid+0.5% lec+200 mM KCl (diamond), and 3% κ-car+80% gs +1.5% lin acid+0.5% lec+200 mM KCl (circle), with the dashed lines indicating the predictions of the mechanical glass transition temperatures.

experimental temperature range of −25 to 0 °C. In the systems with 0.5% or 1% κ-carrageenan and temperatures of −5 and 0 °C, there is a clear depiction of the three-phase lipid oxidation of initiation, propagation and termination. At the low temperature end though (e.g. −25 and −20 °C), systems exhibit mainly the initiation and propagation stages within the experimental confines of observation time in this work. It appears that network formation affects lipid oxidation in these systems. In the presence of 2% κ-carrageenan, for example, the initiation and propagation phases are mainly recorded for all experimental temperatures accompanied by a lower ROOH production, as compared to samples with 0.5 and 1% polysaccharide; similar trends are recorded for the 3% κ-carrageenan blend as well. The significance of the experimental data was confirmed by statistical analysis using a two-way ANOVA test followed by Tukey's post hoc test, which denoted that temperature and level of κ-carrageenan have a significant effect on the ROOH production ($p < 0.05$).

Results encouraged us to calculate oxidation kinetic parameters for these systems using a sigmoidal kinetic model (Farhoosh, 2021; Toorani & Golmakani, 2021). Work started with the zero-order oxidation reaction rate at the initiation phase, which was calculated by fitting experimental data from Fig. 7(a–d) to modelling software (described in the Experimental Analysis Section), using the following equation:

$$\frac{d[ROOH]}{dt} = k_1 \quad (4)$$

where, k_1 refers to the rate constant of the initiation phase.

The rate constant of the initiation phase at different κ-carrageenan concentrations as a function of experimental temperature is illustrated in Fig. 8. It increases continuously reaching the highest values at 0 °C in all treatments, which reflects the significant effect of temperature on oxidation processes. This is due to accelerating chemical reactivity that escalates the rate of hydroperoxide production (Ghnimi, Budilarto, & Kamal-Eldin, 2017). Furthermore, it appears that high levels of the polysaccharide suppress the rate of the oxidation process, as indicated by the lowest value of k_1 obtained for the 3% κ-carrageenan blend (from 0.02 to 0.13 meq kg^{-1} $hours^{-1}$ with increasing temperature), compared to the remaining preparations with 0.5, 1 and 2% κ-carrageenan.

Finally, we estimated the rate constants of pseudo-first-order (k_f) and pseudo-second-order (k_d) reactions that describe the formation and decomposition of ROOH in the propagation phase, respectively. As before, we modelled experimental data from Fig. 7(a–d) using in this occasion the following combination equation:

$$[ROOH] = \frac{k_f}{\exp[k_f(a - t)] + k_d} \quad (5)$$

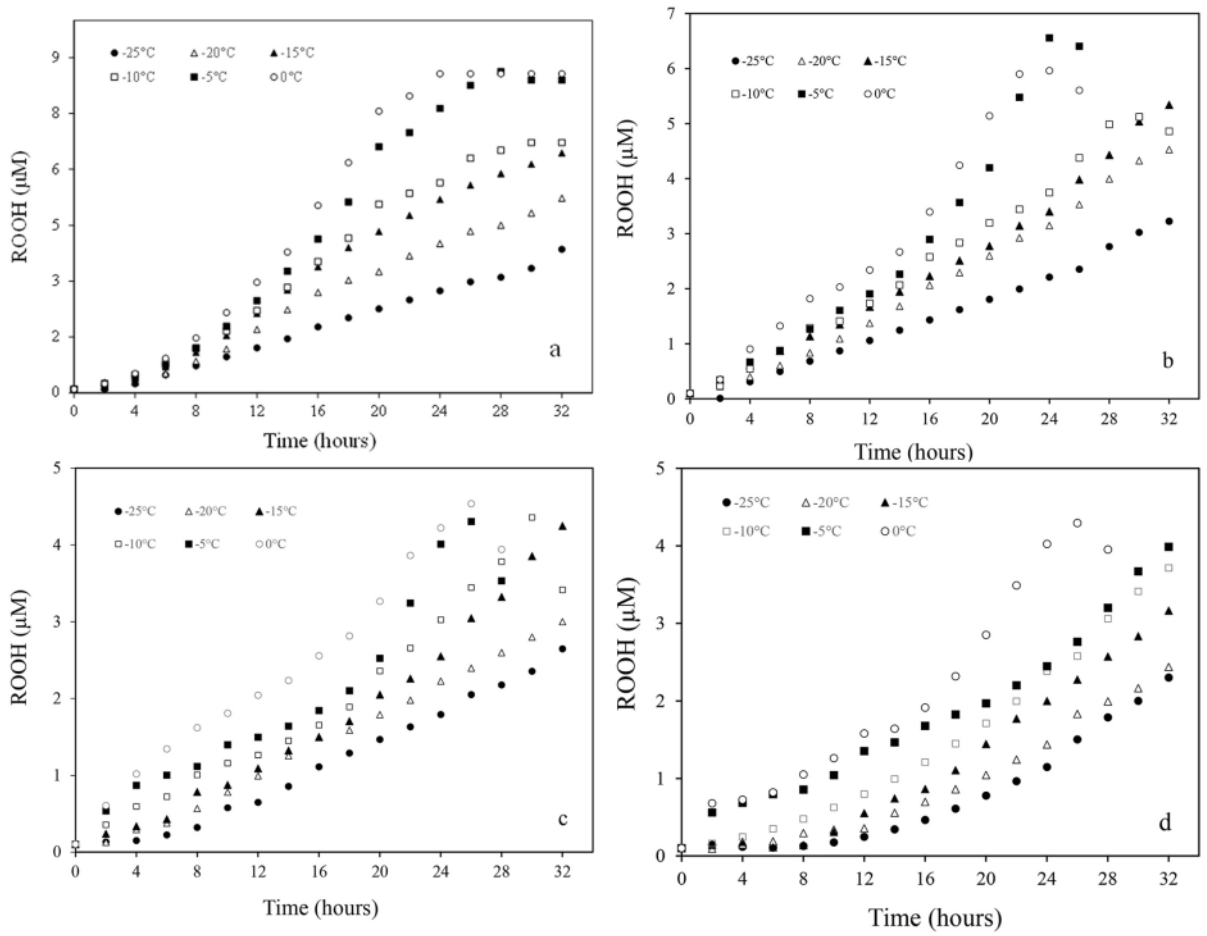

Fig. 7. Hydroperoxide (ROOH) accumulation in the peroxidation of 1.5% linoleic acid in **(a)** 0.5% κ-car+82.5% gs+0.5% lec+200 mM KCl, **(b)** 1% κ-car+82% gs+0.5% lec+200 mM KCl, **(c)** 2% κ-car+81% gs+0.5% lec+200 mM KCl, **(d)** 3% κ-car+80% gs+0.5% lec+200 mM KCl, as a function of the time of observation at −25 (●), −20 (Δ), −15 (▲), −10 (□), −5 (■), 0 (○)°C obtained at 500 nm.

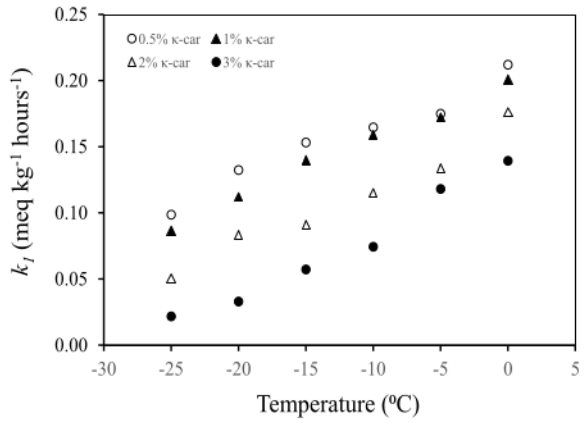

Fig. 8. Rate constant of ROOH formation at the initiation phase (k_1) in 0.5% κ-car+82.5% gs+0.5% lec+200 mM KCl (open circle), 1% κ-car+82% gs+0.5% lec+200 mM KCl (closed triangle), 2% κ-car+81% gs+0.5% lec+200 mM KCl (open triangle), 3% κ-car+80% gs+0.5% lec+200 mM KCl (closed circle) as a function of experimental temperature.

where, a is an overall integration constant, and t is the experimental time.

Derived parameters of ROOH formation and decomposition rates in the propagation phase were utilised to make a correlation with the structural relaxation of our matrices during vitrification, and outcomes are illustrated in Fig. 9(a–d). Throughout experimentation, k_f estimates remain about an order of magnitude higher than those of k_d, indicating a significant formation of hydroperoxides in our systems and experimental protocol. There is also a substantial variation in both parameters with experimental temperature, which show a dramatic drop in the vicinity of the mechanical glass transition temperature. Plotting also shows the temperature gap between T_g and the relatively high estimates of T_{gm} in the κ-carrageenan/glucose syrup/linoleic acid mixture. It clearly demonstrates that the rates of ROOH formation and decomposition have levelled off well before the systems at different concentrations of the polysaccharide reach with controlled cooling the calorimetric glass transition temperature. Hence, it makes the mechanical glass transition temperature a critical parameter in predicting and controlling physicochemical events that occur at the oxidation phase transfer of polyunsaturated fatty acids.

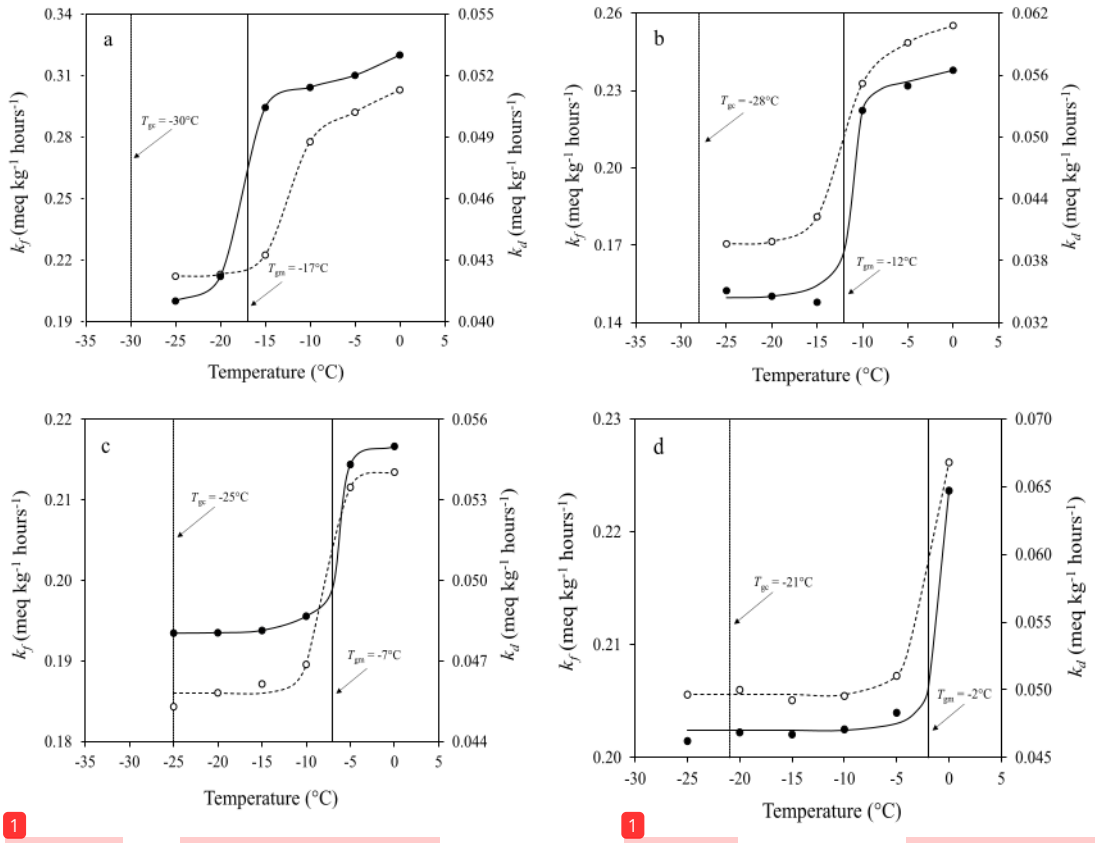

Fig. 9. Rate constant of ROOH formation at the propagation phase (k_f) (◯, left y-axis) and rate constant of ROOH decomposition at the propagation phase (k_d) (●, right y-axis) of 1% linoleic acid in **(a)** 0.5% κ-car+82.5% gs+0.5% lec+200 mM KCl, **(b)** 1% κ-car+82% gs+0.5% lec+200 mM KCl, **(c)** 2% κ-car+81% gs+0.5% lec+200 mM KCl, **(d)** 3% κ-car+80% gs+0.5% lec+200 mM KCl, with indications of the mechanical and calorimetric glass transition temperatures.

4. Conclusions

We designed condensed systems at different concentrations of κ-carrageenan/glucose syrup to carry out studies on the oxidation rate of entrapped linoleic acid. Thus, the rate constants representing the initiation and propagation phases of lipid peroxidation were considered in relation to the structural properties of the polymeric matrix that determine vitrification. It was confirmed that the glass transitions recorded by mechanical measurements occur at much higher temperatures than the calorimetric counterparts thus affording us the opportunity to examine their relevance to lipid peroxidation in these blends. A sigmoidal model was applied successfully to hydroperoxide accumulation data to provide useful indices of lipid susceptibility to oxidation with temperature change and levels of polysaccharide addition in preparations. It was demonstrated that kinetic parameters and rate constants representing the propagation phase in linoleic acid peroxidation are considerably diminished in the vicinity of the mechanical glass transition temperature. As far as we are aware, this is the first time that the utility of T_{gm}, which reflects a barrier effect of the vitrified polymer network on the propagation oxidizability of polyunsaturated fatty acids, is documented for consideration in industrial applications.

Declaration of competing interest

The authors declare that they have no known competing financial interests or personal relationships that could have appeared to influence the work reported in this paper.

CRediT authorship contribution statement

Diah Ikasari: Methodology, Data modeling, Writing – original draft. **Vilia Darma Paramita:** Supervision, Data modeling, Writing – review & editing. **Stefan Kasapis:** Funding acquisition, Conceptualization, Supervision, Writing – review & editing.

Data availability

The authors are unable or have chosen not to specify which data has been used.

Acknowledgements

The authors thank the following institutions and individuals for their contribution to this work: Australia Awards for granting a scholarship to Diah Ikasari, Ms Dyah Andayani for her assistance in modelling lipid oxidation data, and the Australian Microscopy & Microanalysis Research Facility at RMIT University, Australia for experimental support.

Appendix A. Supplementary data

Supplementary data to this article can be found online at https://doi.org/10.1016/j.foodhyd.2023.108555.

References

Arridge, R. G. C. (1975). The glass transition. In R. G. C. Arridge (Ed.), *Mechanics of polymers* (pp. 24–50). Oxford: Clarendon Press.

Cakmak, G., Miller, L. M., Zorlu, F., & Severcan, F. (2012). Amifostine, a radioprotectant agent, protects rat brain tissue lipids against ionising radiation induced damage: An FTIR microspectroscopic imaging study. *Archives of Biochemistry and Biophysics, 520*, 67–73.

Chaudhary, V., Panyoyai, N., Small, D. M., Shanks, R. A., & Kasapis, S. (2017). Effect of the glass transition temperature on alpha-amylase activity in a starch matrix. *Carbohydrate Polymers, 157*, 1531–1537.

Domínguez, R., Pateiro, M., Gagaoua, M., Barba, F. J., Zhang, W., & Lorenzo, J. M. (2019). A Comprehensive review on lipid oxidation in meat and meat products. *Antioxidants, 8*, 429. https://doi.org/10.3390/antiox8100429

Fani, N., Enayati, M. H., Rostamabadi, H., & Falsafi, S. R. (2022). Encapsulation of bioactives within electrosprayed κ-carrageenan nanoparticles. *Carbohydrate Polymers, 294*, Article 119761.

Fan, F., & Roos, Y. H. (2017). Glass transition-associated structural relaxations and applications of relaxation times in amorphous food solids: A review. *Food Engineering Reviews, 9*, 257–270.

Farhoosh, R. (2018). Reliable determination of the induction period and critical reverse micelle concentration of lipid hydroperoxides exploiting a model composed of pseudo-first and -second order reaction kinetics. *LWT - Food Science and Technology, 98*, 406–410.

Farhoosh, R. (2021). Initiation and propagation kinetics of inhibited lipid peroxidation. *Scientific Reports, 11*(1), 1–9.

Ferry, J. D. (1980). *Viscoelastic properties of polymers*. New York: John Wiley & Sons.

Ghnimi, S., Budilarto, E., & Kamal-Eldin, A. (2017). The new paradigm for lipid oxidation and insights to microencapsulation of omega-3 fatty acids. *Comprehensive Reviews in Food Science and Food Safety, 16*, 1206–1218.

Hermansson, A.-M. (1989). Rheological and microstructural evidence for transient states during gelation of kappa-carrageenan in the presence of potassium. *Carbohydrate Polymers, 10*, 163–181.

Hutchinson, J. M. (2009). Determination of the glass transition temperature: Methods correlation and structural heterogeneity. *Journal of Thermal Analysis and Calorimetry, 98*, 579–589.

Ikasari, D., Paramita, V. D., & Kasapis, K. (2022). Glass transition effect on the molecular transport of caffeine from condensed κ-carrageenan/polydextrose systems. *Food Hydrocolloids, 126*, Article 107401.

Kasapis, S. (2006). Definition and applications of the network glass transition temperature. *Food Hydrocolloids, 20*(2), 218–228.

Kasapis, S. (2008). Recent advances and future challenges in the explanation and exploitation of the network glass transition of high sugar/biopolymer mixtures. *Critical Reviews in Food Science and Nutrition, 48*, 185–203.

Kasapis, S. (2012). Relation between the structure of matrices and their mechanical relaxation mechanisms during the glass transition of biomaterials: A review. *Food Hydrocolloids, 26*(2), 464–472.

Kasapis, S., Al-Marhoobi, I. M., & Mitchell, J. R. (2003). Testing the validity of comparisons between the rheological and the calorimetric glass transition temperatures. *Carbohydrate Research, 338*(8), 787–794.

Kibar, E. A. A., Gönenç, İ., & Us, F. (2014). Effects of fatty acid addition on the physicochemical properties of corn starch. *International Journal of Food Properties, 17*(1), 204–218. https://doi.org/10.1080/10942912.2011.619289

Kontogiorgos, V., & Kasapis, S. (2017). Modeling and fundamental aspects of structural relaxation in high-solid hydrocolloid systems. *Food Hydrocolloids, 68*, 232–237.

Linke, A., Weiss, J., & Kohlus, R. (2020). Oxidation rate of the non-encapsulated- and encapsulated oil and their contribution to the overall oxidation of microencapsulated fish oil particles. *Food Research International, 127*, Article 108705.

Ma, U. V. L., Floros, J. D., & Zieger, G. R. (2011). Formation of inclusion complexes of starch with fatty acid esters of bioactive compounds. *Carbohydrate Polymers, 83*, 1869–1878.

Marangoni, F., Agostoni, C., Borghi, C., Catapano, A. L., Cena, H., Ghiselli, A., … Polia, A. (2020). Dietary linoleic acid and human health: Focus on cardiovascular and cardiometabolic effects. *Atherosclerosis, 292*, 90–98.

Nogueira, M. S., Scolaro, B., Milne, G. L., & Castro, I. A. (2019). Oxidation products from omega-3 and omega-6 fatty acids during a simulated shelf life of edible oils. *LWT - Food Science and Technology, 101*, 113–122.

Orlien, V., Andersen, A. B., Sinkko, T., & Skibsted, L. H. (2000). Hydroperoxide formation in rapeseed oil encapsulated in a glassy food model as influenced by hydrophilic and lipophilic radicals. *Food Chemistry, 68*, 191–199.

Panyoyai, N., Bannikova, A., Small, D. M., & Kasapis, S. (2015). Controlled release of thiamin in a glassy κ-carrageenan/glucose syrup matrix. *Carbohydrate Polymers, 115*, 723–731.

Paramita, V. D., Bannikova, A., & Kasapis, S. (2015). Release mechanism of omega-3 fatty acid in κ-carrageenan/polydextrose undergoing glass transition. *Carbohydrate Polymers, 126*, 141–149.

Paramita, V. D., Bannikova, A., & Kasapis, S. (2016). Preservation of oleic acid entrapped in a condensed matrix of high-methoxy pectin with glucose syrup. *Food Hydrocolloids, 53*, 284–292.

Paramita, V. D., Lo Piccolo, J. D., & Kasapis, S. (2017). Effect of co-solute concentration on the diffusion of linoleic acid from whey protein matrices. *Food Hydrocolloids, 70*, 277–285.

Rahman, M. S. (2009). Food stability beyond water activity and glass transition: Macro-micro region concept in the state diagram. *International Journal of Food Properties, 12*, 726–740.

Saini, R. K., & Keum, Y. (2018). Omega-3 and omega-6 polyunsaturated fatty acids: Dietary sources, metabolism, and significance – a review. *Life Sciences, 203*, 255–267.

Salcedo-Sandoval, L., Cofrades, S., Ruiz-Capillas, C., Matalanis, A., McClements, D. J., Decker, E. A., et al. (2015). Oxidative stability of n-3 fatty acids encapsulated in filled hydrogel particles and of pork meat systems containing them. *Food Chemistry, 184*, 207–213.

Thrimawitana, T. R., Young, S., Dunstan, D. E., & Alany, R. G. (2010). Texture and rheological characterisation of kappa and iota carrageenan in the presence of counter ions. *Carbohydrate Polymers, 82*, 69–77.

Toorani, M. R., & Golmakani, M. T. (2021). Investigating relationship between water production and interfacial activity of γ-oryzanol, ethyl ferulate, and ferulic acid during peroxidation of bulk oil. *Scientific Reports, 11*, Article 17026. doi.org/10.1038/s41598-021-96439-9.

Webber, V., Carvalho, S. M. D., Ogliari, P. J., Hayashi, L., & Barreto, P. L. M. (2012). Optimisation of the extraction of carrageenan from Kappaphycus alvarezii using response surface methodology. *Food Science and Technology, 32*, 812–818.

Yang, L., & Paulson, A. T. (2000). Effects of lipids on mechanical and moisture barrier properties of edible gellan film. *Food Research International, 33*, 571–578.

B1 paper

ORIGINALITY REPORT

9%	9%	11%	2%
SIMILARITY INDEX	INTERNET SOURCES	PUBLICATIONS	STUDENT PAPERS

PRIMARY SOURCES

1	assets.researchsquare.com Internet Source	2%
2	Paul George, Leif Lundin, Stefan Kasapis. "Effect of thermal denaturation on the mechanical glass transition temperature of globular protein/co-solute systems", Food Hydrocolloids, 2014 Publication	1%
3	Nazim Nassar, Felicity Whitehead, Taghrid Istivan, Robert Shanks, Stefan Kasapis. "Manipulation of the Glass Transition Properties of a High-Solid System Made of Acrylic Acid-N,N'-Methylenebisacrylamide Copolymer Grafted on Hydroxypropyl Methyl Cellulose", International Journal of Molecular Sciences, 2021 Publication	1%
4	docksci.com Internet Source	1%
5	Jiang, Bin, and Stefan Kasapis. "Kinetics of a Bioactive Compound (Caffeine) Mobility at the	1%

Vicinity of the Mechanical Glass Transition Temperature Induced by Gelling Polysaccharide", Journal of Agricultural and Food Chemistry, 2011.
Publication

---

6 Naksit Panyoyai, Anna Bannikova, Darryl M. Small, Robert A. Shanks, Stefan Kasapis. "Diffusion of nicotinic acid in spray-dried capsules of whey protein isolate", Food Hydrocolloids, 2016
Publication

1 %

---

7 eprints.hud.ac.uk
Internet Source

1 %

---

8 Stefan Kasapis, Insaf M. Al-Marhoobi, John R. Mitchell. "Testing the validity of comparisons between the rheological and the calorimetric glass transition temperatures", Carbohydrate Research, 2003
Publication

1 %

---

9 Lorena Salcedo-Sandoval, Susana Cofrades, Claudia Ruiz-Capillas, Alison Matalanis et al. "Oxidative stability of n-3 fatty acids encapsulated in filled hydrogel particles and of pork meat systems containing them", Food Chemistry, 2015
Publication

1 %

---

10 a434.tongji.edu.cn
Internet Source

1 %
